Astron. Astrophys. 350, 1079–1084 (1999)

ASTRONOMY AND ASTROPHYSICS

An improved model of the seasonal Yarkovsky force for regolith–covered asteroid fragments

David Vokrouhlický and Miroslav Brož

Institute of Astronomy, Charles University, V Holešovičkách 2, 180 00 Prague 8, Czech Republic
(vokrouhl@mbox.cesnet.cz; mira@sirrah.troja.mff.cuni.cz)

Received 13 April 1999 / Accepted 27 August 1999

Abstract. We derive a new analytical solution for the seasonal Yarkovsky effect, the mean–motion frequency mode of the recoil force due to reradiated sunlight, on a spherical asteroid fragment. The body is assumed to have a thin low–conductivity (regolith–like) surface layer, covering a much more thermally conductive core. If the penetration depth of the seasonal thermal wave in the low–conductivity surface material is larger than the regolith's geometrical thickness, the previous simplified solution assuming a homogeneous interior of the body might lead to wrong estimates on the intensity of the perturbing force. Our approach removes this problem and the results indicate: (i) an increased seasonal mobility of 10–m sized and larger fragments with an insulating surface layer, and (ii) a decreased seasonal mobility of meter–sized fragments with the same structure. These results may affect the accuracy of simulations of meteorite and NEA transport to the Earth, as well as the dynamical evolution of some real small asteroids (e.g. 1566 Icarus).

Key words: celestial mechanics, stellar dynamics – minor planets, asteroids

1. Introduction

Thermal phenomena on asteroid fragments have attracted considerable attention over the last few years, since their dynamical aspects, known as the Yarkovsky effects, have been found to be important in solving some interesting problems related to the transport of NEAs and meteoroids to the Earth vicinity (e.g. Farinella et al. 1998; Hartmann et al. 1999, Vokrouhlický & Farinella 1998; Farinella & Vokrouhlický 1999; Bottke et al. 1999). A quantitative understanding of the astronomical role of the Yarkovsky effects requires: (i) a reliable knowledge of the thermal and other parameters affecting their efficiency (e.g., the surface thermal conductivity of asteroid fragments, collisional evolution time scales, etc.), and (ii) a realistic modelling of the thermal effects themselves. Whereas the former problem basically requires observational inputs (such as thermal–IR observations of asteroid surfaces during fly–by space missions), the latter demands theoretical efforts. Among the issues to be investigated one can mention the role of non–spherical shapes (see Vokrouhlický 1998b and Vokrouhlický & Farinella 1998 for some preliminary results), the effects of fractures running through the body, and the emission properties of the body's surface (including those due to surface roughness and the directional properties of the emission lobe, improving on the simple Lambert–law isotropic geometry which has been always assumed so far in the framework of Yarkovsky force studies).

In this note we aim to extend the applicability of the existing thermal models by taking into account another problem, namely the possible inhomogeneity of the thermal parameters in the bodies. A related problem in radiometry has been studied by Brown & Matson (1987), who have investigated the role of the finite propagation depth for insolation on a porous asteroid surface. In this paper, we shall focus on modelling the thermal effects for bodies which have a layered structure: a highly–conductive core covered by a thin layer of a low–conductivity material (such as a porous, dusty or finely fragmented regolith).

This problem is interesting for the following reasons, which are different for the diurnal and the seasonal components of the Yarkovsky effect. In the case of the seasonal effect, which has been recently analyzed for a range of surface thermal conductivities including the very low values appropriate for regoliths (Rubincam 1995, Farinella et al. 1998), the penetration depth l_s of the seasonal thermal wave for a body covered by low–conductivity, regolith–like surface material would be of about 15 cm. Because the corresponding penetration depth is much larger for compact rocky material, due to its higher thermal conductivity (e.g. $l_s \approx 2$ m for a bare–rock basalt surface) the seasonal temperature changes would affect a much larger fraction of the body's volume than just the surface layer if the latter were thinner than the corresponding value of l_s and the underlying core were much more conductive. In such a case, the temperature gradient across the body and the resulting Yarkovsky effect would be very different with respect to the values predicted by assuming a homogeneous structure, having the same conductivity throughout the interior as on the surface.

Modelling the diurnal component of the Yarkovsky effect for bodies with very low surface conductivity presents a different problem. Using the thermal parameters measured for the lunar regolith (e.g. Langseth et al. 1973), we obtain an estimate of $38.3/\sqrt{\omega}\,\mu\mathrm{m}$ for the penetration depth of the diurnal

Send offprint requests to: D. Vokrouhlický

thermal wave (here ω is the rotation frequency of the body in rad/s). Assuming a linear dependence of the rotation period P on mean radius R of the body, such as $P = (2\pi/\omega) = 5\,R$ (with R in meters; this is the relationship recently adopted for asteroid fragments by Farinella & Vokrouhlický 1999), we can express the estimated diurnal penetration depth as a function of the body's size: $34.2\,\sqrt{R}\ \mu\mathrm{m}$. For the meter–sized bodies of interest in meteoritics this depth is submillimetric. Since on this scale the surface is likely to be dusty or particulate, with a complex mixture of micrometric grains and voids of similar size, the current models based on the homogeneity assumption are very likely to be simplistic. If the surface microparticles are optically thin, the impinging radiation may penetrate to some depth in the body and represent effectively an additional source of energy (see e.g. Brown & Matson 1987). However, dealing with this problem is much more complicated than in the previously mentioned case of the seasonal effect, and in this paper we will limit ourselves to the latter.

Coming back to the regolith issue, is it plausible to assume that small (say, meter–sized) asteroid fragments or meteoroids have a thin, low–conductivity surface layer? In our opinion, the available observational evidence allows no definite reply for the time being. Meteorites are normally covered by a fusion crust developed during their passage through the Earth's atmosphere and their original surface material cannot be observed; recent studies of these fusion crusts (Genge & Grady 1999) indicate that their compositions are similar to those of the bulk meteorites, both at the same time suggest that meteorite ablation spheres produced at high altitudes resemble cosmic spherules derived from coarse-grained precursors. It is also interesting to note, in this respect, that many fireballs show anomalous ablation efficiencies and/or IR luminosities already at very high altitudes, a possible explanation of which would be the early loss of loose surface material (Z. Ceplecha, private communication). As for larger bodies, surface regolith has been observed on asteroids such as Gaspra and Ida; recently, the presence of a meter–thick dust coating on the Martian moon Phobos has been inferred from the large temperature differences (more than 100 K) between the day and night sides of this satellite, measured by the Mars Global Surveyor thermal emission spectrometer instrument (see e.g. http://www.newmars.com/). This case is particularly interesting because most of Phobos's surface overflows its Roche lobe (Dobrovolskis & Burns 1980), and despite this the near–surface dust particles have not been flung off – an indication that electrostatic interactions (see e.g. Lee 1996) may keep dust or fine fragments sticking on the surface despite the centrifugal force due to the presumably rapid rotation of small bodies. In this regard, we stress that the theory discussed in the remainder of this paper is not meant to be applied only in the case of real regoliths, formed by ejecta from relatively large–scale impacts, but also to bodies whose surface material may have developed a certain degree of porosity or granularity, e.g. because of micrometeorite impacts. Measurements of Wechsler et al. (1972), Presley & Christensen (1997) and Yomogida & Matsui (1983) show that such porous or particulate materials have thermal conductivities much lower (even by two or three orders of magnitude) than compact rocks, including most meteorite samples used by Yomogida & Matsui. In conclusion, we think that the the possibility of a layered structure for small asteroids/meteoroids cannot be ruled out at this time, and therefore it is worth some modelling effort.

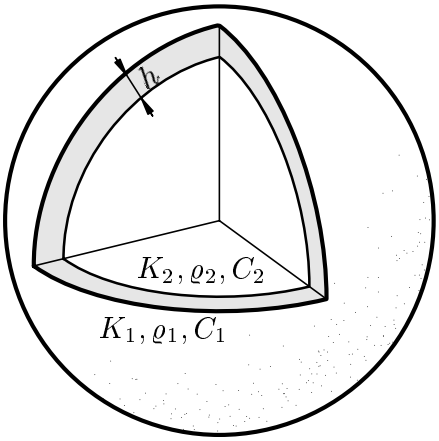

Fig. 1. The interior structure of a layered body as discussed in the text.

In this note, we consider the seasonal Yarkovsky effect only and remove the homogeneity assumption adopted in the previous thermal models, by considering bodies with a simple layered structure. Sect. 2 is devoted to the derivation of the semimajor axis drift rate in this case from a linearized thermal theory, while in Sect. 3 we discuss some specific examples and applications and draw some conclusions on the importance of this issue.

2. Theory

Hereinafter we shall use the same mathematical approach and, to a large extent, the same notations introduced in the series of papers by Vokrouhlický (1998a,b; 1999). The reader is referred to these papers for further details.

We are going to derive a linearized solution for the temperature variations in a spherical and rotating body, that revolves around a radiating source (the Sun in our case) in a circular orbit. The body, of radius R, is assumed to have a thin and homogeneous surface layer of thickness h, characterized by thermal conductivity K_1, thermal capacity C_1 and density ρ_1. The corresponding parameters for the underlying core are K_2, C_2 and ρ_2. We assume that the thermal conductivities K_1 and K_2 are different; typically, $\xi_2 \equiv K_1/K_2 \leq 1/100$. For later use we also introduce the ratio between the thermal depths in the two parts of the body, $\xi_1 \equiv \sqrt{K_1\rho_2C_2/K_2\rho_1C_1} \leq 1/15$. Fig. 1 shows the geometrical structure of the bodies discussed in this note.

Since we shall use a linearized heat conduction theory, the temperature T throughout the body is assumed to oscillate around a constant mean value T_{av}: $T = T_{\mathrm{av}} + \Delta T$. The constant average part is defined by the formal conservation of absorbed and reradiated energy, without taking into account the heat conduction effects. The heat conduction problem then requires one to solve for the temperature variation ΔT at any time

t everywhere in the body. The volume elements in the body are labelled by their spherical coordinates $(r;\theta,\phi)$.

A suitable scaling of the variables simplifies the mathematical formulation of the problem. The radial coordinate r is scaled by the thermal penetration depth $l_s^1=\sqrt{K_1/\rho_1 C_1 n}$ of the surface layer: $r\to r'=r/l_s^1$ (scaled quantities are denoted by a prime; n is the mean motion of the orbital revolution around the Sun). The temperature variation ΔT is scaled by the subsolar surface temperature $T_\star$, defined from $\epsilon\sigma T_\star^4=\alpha\mathcal{E}_\star$ (ϵ is the thermal emissivity and α the optical absorption coefficient of the surface, σ the Stefan–Boltzmann constant and $\mathcal{E}_\star$ the solar radiation flux at the body's distance from the Sun). Finally, time t is replaced by the complex variable $\zeta=\exp(i\lambda)$, where $\lambda=n(t-t_0)$ is the mean longitude along the orbit. The time origin t_0 is chosen in such a way that the solar colatitude θ_0 in the body's reference frame (measured from the body's spin axis) fulfils the condition $\cos\theta_0=\sin\gamma\sin\lambda$ (here γ is the obliquity of the spin axis).

The linearized heat conduction problem then satisfies the Fourier equation (see e.g. Vokrouhlický 1998a; 1999):

$$i\zeta\frac{\partial}{\partial\zeta}\ \Delta T'(r';\theta,\phi;\zeta)= \tag{1}$$
$$=\ \frac{1}{r'^2}\left\{\frac{\partial}{\partial r'}\left(r'^2\frac{\partial}{\partial r'}\right)+\Lambda\left(\theta,\phi\right)\right\}\ \Delta T'(r';\theta,\phi;\zeta)\ ,$$

where the operator $\Lambda(\theta,\phi)$ is given by

$$\Lambda\left(\theta,\phi\right)=\frac{1}{\sin\theta}\left[\frac{\partial}{\partial\theta}\left(\sin\theta\frac{\partial}{\partial\theta}\right)+\frac{1}{\sin\theta}\frac{\partial^2}{\partial\phi^2}\right]\ . \tag{2}$$

The general solution of Eq. (1) is constrained by three boundary conditions. The energy flux conservation at the body's surface ($r'=R'$) reads

$$\sqrt{2}\Delta T'(R')+\Theta\left[\frac{\partial\Delta T'(R')}{\partial r'}\right]=\Delta\mathcal{E}'\ , \tag{3}$$

with the incident radiation flux $\mathcal{E}$ normalized by the "subsolar" value $\mathcal{E}_\star$ ($\mathcal{E}'=\mathcal{E}/\mathcal{E}_\star$) and $\Theta=\sqrt{K_1\rho_1C_1}\sqrt{n}/\epsilon\sigma T_\star^3$ defined as the seasonal thermal parameter of the surface low–conductivity layer. The boundary condition (3) depends on the particular surface element (θ,ϕ) and time (ζ) that are considered. The right–hand side term in Eq. (3) ($\Delta\mathcal{E}'=\mathcal{E}'-\frac{1}{4}$) can be developed in a spherical harmonics series

$$\Delta\mathcal{E}'=\sum_{n\geq1}\sum_{k=-n}^{n}\varepsilon_{nk}(\zeta)\,Y_{nk}(\theta,\phi)\ , \tag{4}$$

where only the dipole zonal term will be relevant below. Vokrouhlický (1999) has showed that the corresponding amplitude $\varepsilon_{10}(\zeta)$ is

$$\varepsilon_{10}(\zeta)=\frac{1}{2i}\sqrt{\frac{\pi}{3}}\ \sin\gamma\left(\zeta-\zeta^{-1}\right)\ . \tag{5}$$

A new type of constraint in this case is due to the boundary between the surface layer and the core (at $r'=R'-h'$), which are assumed to be in perfect thermal contact (see e.g. Boley & Weiner 1960). Both the temperature and the heat flux are to be continuous on this surface, and therefore

$$\Delta T'(R'-h')_+\ =\ \Delta T'(R'-h')_-\ , \tag{6}$$
$$\xi_2\left[\frac{\partial\Delta T'(R'-h')}{\partial r'}\right]_+\ =\ \left[\frac{\partial\Delta T'(R'-h')}{\partial r'}\right]_-\ . \tag{7}$$

The indexes $\pm$ indicate that the corresponding quantities have to be computed as a limit ($r'\to R'-h'$) from the surface layer ($+$) or the core ($-$) region.

Thanks to the spherical geometry, the temperature distribution in the body can be developed as a spherical harmonics series

$$\Delta T'(r';\theta,\phi;\zeta)=\sum_{n\geq1}\sum_{k=-n}^{n}t'_{nk}(r';\zeta)\,Y_{nk}(\theta,\phi)\ , \tag{8}$$

with the coefficients $t'_{nk}(r';\zeta)$ depending on the scaled radial distance r' from the center and time ζ. Only the dipole part $t'_{10}(r';\zeta)$ is required to compute the seasonal Yarkovsky acceleration $\mathbf{a}$ (see Vokrouhlický 1999), since

$$\mathbf{a}(\zeta)=-\frac{4}{3}\sqrt{\frac{2}{3\pi}}\,\alpha\Phi\,t'_{10}(R';\zeta)\,\mathbf{s}\ . \tag{9}$$

Here, $\mathbf{s}$ is the unit vector in the direction of the spin axis and $\Phi=\pi R^2\mathcal{E}_\star/mc$ is the usual radiation pressure factor (m is the mass of the body and c the velocity of light). Like in the simpler case of thermal effects on a homogeneous body (e.g. Rubincam 1998; Vokrouhlický 1999), the $t'_{10}(r';\zeta)$ coefficient satisfies a Bessel equation in both the surface layer and the core. In the core, the solution depends only on the spherical Bessel function of the first kind (in order to guarantee regularity at $r'=0$), whereas in the surface layer the solution in general is a mixture of the two fundamental solutions (of first and second kind) of the Bessel equation.

After a great deal of algebra we obtain

$$t'_{10}(R';\zeta)=\sqrt{\frac{\pi}{6}}\ \sin\gamma\,\frac{E_{R'}\sin(\lambda+\delta_{R'})}{1+\chi}\ , \tag{10}$$

where

$$E_{R'}\exp(i\delta_{R'})=\frac{\beta_4-\beta_3}{\beta_1\beta_4-\beta_2\beta_3}\ . \tag{11}$$

The auxiliary complex β–factors are given by

$$\beta_1\ =\ 1+\frac{\chi}{1+\chi}\psi_1(z_1)\ , \tag{12}$$
$$\beta_2\ =\ 1-\frac{3\chi}{1+\chi}+\frac{\chi}{1+\chi}\psi_2(z_1)\ , \tag{13}$$
$$\beta_3\ =\ \left[\xi_2-1+\xi_2\psi_1\left(z_2\right)-\psi_1\left(z_3\right)\right]\ \psi_3\left(z_2\right)\ , \tag{14}$$
$$\beta_4\ =\ \left[-2\xi_2-1+\xi_2\psi_2\left(z_2\right)-\psi_1\left(z_3\right)\right]\ \psi_3\left(z_1\right)\ , \tag{15}$$

with

$$\psi_1(z)\ =\ \frac{z}{j_1(z)}\frac{dj_1(z)}{dz}-1\ , \tag{16}$$
$$\psi_2(z)\ =\ \frac{z}{n_1(z)}\frac{dn_1(z)}{dz}+2\ , \tag{17}$$
$$\psi_3(z)\ =\ \frac{j_1(z)}{n_1(z)}\ . \tag{18}$$

Here, $j_1(z)$ and $n_1(z)$ are the spherical Bessel functions of the first and the second kind. The complex arguments of the β functions read: $z_1 = \sqrt{-i}\,R'$, $z_2 = \sqrt{-i}\,(R'-h')$ and $z_3 = \sqrt{-i}\,\xi_1(R'-h')$. Finally, the real parameter χ is defined by: $\chi = \Theta/\sqrt{2}R'$.

Finally, using the corresponding Gauss perturbation equation we can estimate the secular rate of the orbital semimajor axis:

$$\frac{da}{dt} = \frac{4\alpha}{9}\,\frac{\Phi}{n}\,\frac{E_{R'}\sin\delta_{R'}}{1+\chi}\,\sin^2\gamma\;. \qquad (19)$$

This result is formally identical to Eq. (26) in Vokrouhlický (1999), which had been derived for a homogeneous spherical body. However, in our case the amplitude $E_{R'}$ and the seasonal thermal phase lag $\delta_{R'}$ are given by the much more complex expressions (11) – (18) derived above (see Appendix A for a numerical method suitable for the evaluation of the $E_{R'}\,\sin\delta_{R'}$ factor when $R' \gg 1$). Obviously, taking the limit for a homogeneous body (i.e. $K_1 = K_2$, $\rho_1 = \rho_2$ and $C_1 = C_2$) the semimajor axis secular drift (19) reduces to the simpler result (26) in Vokrouhlický (1999). The same applies for the limit $h \to R$, when the surface layer formally extends over the whole body, and the limit $h \to 0$, when the surface layer disappears.

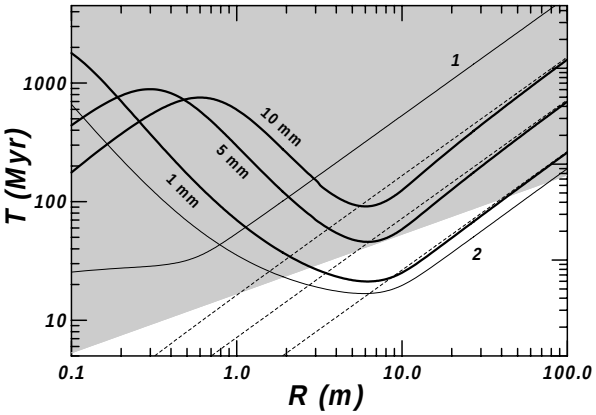

Fig. 2. The average time (in Myr) required to move an asteroid fragment by 0.05 AU in semimajor axis through the seasonal variant of the Yarkovsky effect is plotted vs. the body's radius R (in meters). The solutions of this paper for three thicknesses h of the low–K layer (thick solid lines: $h = 1$ mm, $h = 5$ mm, $h = 10$ mm) are compared with the simplified solutions for a homogeneous body (thin solid lines: curve 1 for $K_1 = 0.0015$ W/m/K, corresponding to the low–K surface layer; curve 2 for $K_2 = 1$ W/m/K, corresponding to the highly conductive core). The asymptotic behaviors, based on the solutions of the 1–D heat diffusion problem (see Appendix B), are shown by the dashed lines. Timescales longer than the estimated collisional lifetimes of the fragments correspond to the shaded upper region.

3. Examples and conclusions

In order to assess the importance of the effects related to the possible layered structure of asteroid fragments, we have performed two tests. In both of them we assume the following parameters: (i) $K_1 = 0.0015$ W/m/K and $\rho_1 = 1.5$ g/cm^3 for the low–K surface layer, and (ii) $K_2 = 1$ W/m/K and $\rho_2 = 3.5$ g/cm^3 for the high–K core.

First, we have estimated the timescale required to move a main–belt body by 0.05 AU due to the seasonal Yarkovsky effect, assuming a body initially at $a = 2.25$ AU (for a similar discussion see Hartmann et al. 1999). The statistical method of Farinella & Vokrouhlický (1999) was used to include the effects of random changes in the spin axis orientation due to collisions with the background population of main–belt bodies. The results, shown in Fig. 2, indicate that the previous, simplified approach (assuming a homogeneous low–K body) overestimates in a significant way the seasonal effect mobility of meter–sized, regolith–covered fragments, while at the same time it significantly underestimates the seasonal effect mobility bodies with the same structure in 10 to 100 m size range. On the other hand, assuming a high–K homogeneous structure would overestimate the seasonal Yarkovsky drift rate over all the size range exceeding a few tens of cm.

These results are easy to understand. We recall that the assumed geometrical thickness of the regolith–layer (up to 10 mm in Fig. 2) is smaller than the penetration depth l_s^1 (about 15 cm) of the seasonal thermal wave corresponding to the thermal parameters of this material. The surface temperature variations thus penetrate well into the highly conductive core of the body. Since the typical penetration depth l_s^2 of the seasonal thermal wave in the core is of the order of $1-3$ m, the efficient heat conduction through the interior of the meter–sized body results in a significant decrease of its thermal gradients and semimajor axis mobility. In other words, the effect of the highly conductive core helps the temperature to get closer to an average value and thus decreases the efficiency of the seasonal Yarkovsky effect. On the other hand, the higher conductivity of the core also helps in increasing the "average" thermal parameter (indicating roughly how much the thermal reemission lags behind the absorption of sunlight) in the case of 10 m sized and larger bodies. This effect then leads to a faster seasonal Yarkovsky mobility compared to low–K homogeneous bodies in this size range, as illustrated in Fig. 2.

Fig. 3 shows the average semimajor axis drift of asteroid fragments of different sizes within their estimated collisional lifetimes (compare with Fig. 3 in Farinella & Vokrouhlický 1999). The more efficient mobility of fragments around 10 m in radius when they are covered by a poorly conductive surface layer is confirmed here [see the bump on the thick curves in strip (b)]. Bodies of this size have both a high diurnal effect mobility and, on top of this, a significantly increased seasonal effect mobility (as discussed above). We recall that thanks to the very small penetration depth of the diurnal thermal wave (see Sect. 1), the previous models for the diurnal effect remain essentially correct – unless, of course, the granularity effects mentioned in Sect. 1 play an important role.

Let us now comment briefly on the possible astronomical relevance of the enhanced (for "large" bodies) or inhibited (for "small" bodies) seasonal Yarkovsky mobility resulting from the effect analysed in this paper.

First, the increased semimajor axis mobility of bodies around 10 m in size, when they have a thin, low–conductivity

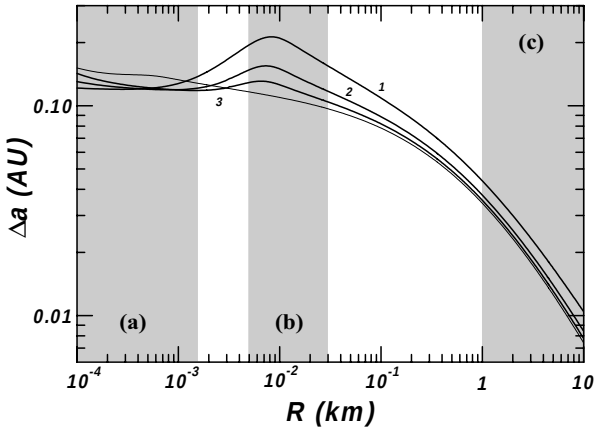

Fig. 3. Average semimajor axis drift (in AU) within the lifetime of an asteroid fragment vs. its radius R (in km). Both diurnal and seasonal effects are included here. The assumed collisional lifetime of $16.8\,\sqrt{R}$ Myr is taken from Farinella & Vokrouhlický (1999). The complete solution of the seasonal effect (as derived in this paper) is shown for three thicknesses of the low–K layer (thick solid lines: curve 1 for $h = 1$ mm; curve 2 for $h = 5$ mm; curve 3 for $h = 10$ mm) and is compared to the simplified solution for a homogeneous body whose thermal parameters correspond to the surface layer (thin solid line). The diurnal variant of the Yarkovsky effect is the same in all cases. Region (b) of the figure, where the largest differences are found, corresponds to Tunguska–like Earth impactors with typical diameters of 10 – 60 m. Regions (a) and (c) correspond to the size ranges characteristic of meteorites and large NEAs, respectively, as discussed by Farinella & Vokrouhlický (1999).

surface layer, could enhance the flux of these bodies into the main–belt resonances. Their overabundance in the resonances should then result in a corresponding excess among the Earth–crossing objects. Rabinowitz's (1993, 1994) analysis of Spacewatch survey data indicates that such an excess exists in the observed NEA population, and several authors (Rubincam 1995; Hartmann et al. 1999; Vokrouhlický & Farinella 1999a) have suggested the relatively high Yarkovsky mobility of these bodies as a plausible explanation. Future quantitative simulations on the transport and "demography" of NEAs of different sizes should take into account Yarkovsky effects in the best possible way, including the implications of the improved thermal model discussed here, in particular in the critical diameter range between about 10 and 50 m.

Second, the quantitative results on the expected cosmic ray exposure ages of different types of meteorites recently obtained by Vokrouhlický & Farinella (1999b) by a Monte Carlo model depend on the mobility of asteroid fragments in the critical size range around 10 m. The reason is that the model indicates that most meteorites reach the Earth after a cascade of successive fragmentation events (as already suggested by Wetherill 1985), and the 10–m objects often are the immediate precursors of the recovered meteorites. What is the abundance of these bodies in the main belt, do they often succeed in reaching the resonances before being broken up, how many are disrupted *en route* to the Earth, are all open questions at present, and the replies may depend upon the assumed thermal models.

Let us consider, for instance, a 10 m sized, regolith–covered body released at a 0.15 AU distance from a resonance in the inner region of the asteroid belt – this is roughly the case of ejecta from asteroid Vesta, the best candidate parent body for the HED meteorites. Using the results shown in Fig. 3, we can see that the simplified (homogeneous) thermal model predicts a typical drift of about 0.1 AU within the estimated lifetime of a 10 m body, which would not be sufficient to reach the resonances for many fragments released from Vesta. However, when the model developed here is used instead, the enhanced mobility may protect most 10 m bodies from being disrupted on their way to the resonances, thus inhibiting to some extent the importance of the collisional cascade effects.

A detailed analysis of the orbital dynamics of the near–Earth asteroid (1566) Icarus represents a special problem where the results of this paper might provide an element of the solution. According to Sitarski (1991), Icarus's orbit determination reveals an unexplained secular semimajor axis decrease of about 7.5×10^{-4} AU/Myr. Given the fact that Icarus, which is about ≈ 900 m in diameter, could well have a regolith cover, the results reported above suggest that in modelling the seasonal Yarkovsky effect on this body the homogeneity assumption might lead to wrong estimates (an additional difficulty is that Icarus's orbit is very eccentric, and that also poses a special problem for the evaluation of the seasonal Yarkovsky effect). Indeed, preliminary attempt to model the Yarkovsky semimajor axis drift for Icarus's orbit (Vokrouhlický, in preparation) indicates that the current models fail to predict the observed value as reported by Sitarski (1991). Of course, there are some simple possible explanations this discrepancy, such as: (i) Sitarski's value is overestimated [e.g., Yeomans (1992) was unable to confirm Sitarski's result]; (ii) Icarus is smaller than it was assumed. However, the possibility should also be considered that the seasonal Yarkovsky effect has been somewhat underestimated due to the simplifying assumptions of the current thermal models, and a fully numerical model that would simulate consistently the abrupt change in the thermal conductivity at the boundary between the two layers (but extending to the nonlinear regime the linearized analysis of this paper) is required to obtain more accurate results. Although this possibility seems plausible to us, we must await a detailed re–analysis of Icarus's orbit for a realistic assessment. In any case, Icarus's dynamics might offer a unique test of the Yarkovsky effect on such a large, natural orbiting body.

Acknowledgements. The authors thank P. Farinella for helpful discussions and assistance in revising the paper. They are also grateful to the reviewer, D.P. Rubincam, for some criticism which was useful to clarify the final version of the paper.

Appendix A: numerical evaluation of Eq. (11)

In this appendix we comment on the numerical evaluation of the complex function $E_{R'} \exp(i\delta_{R'})$ in Eq. (11), which is an important step in the procedure to estimate the semimajor axis drift (19). Curiously, this problem is rather tricky, for reasons that will be explained below.

First, a more suitable representation of Eq. (11) reads

$$E_{R'} \exp(i\delta_{R'}) = \frac{1}{\beta_1 + \beta_3 \frac{\beta_1-\beta_2}{\beta_4-\beta_3}} \ . \tag{A1}$$

where the ratio of the β functions in the second term of the denominator is of particular concern. Using simple algebraic identities for the spherical Bessel functions, one proves that

$$\beta_1 - \beta_2 = \frac{\chi}{1+\chi} \frac{z_1}{\psi_3(z_1)} \frac{d\psi_3(z_1)}{dz} \ . \tag{A2}$$

More cumbersome algebra then leads to

$$\begin{aligned} \beta_4 - \beta_3 \ = \ & -z_1 \frac{d\psi_3(z_1)}{dz} \left[\xi_2 + \frac{h}{R} \alpha_1 (z_1; R, \xi_1, \xi_2) \right. \\ & \left. + \left(\frac{h}{R}\right)^2 \alpha_2 (z_1; R, \xi_1, \xi_2) + \ldots \right] , \end{aligned} \tag{A3}$$

where α_1, α_2, etc. are some complex functions. Note that both $(\beta_1 - \beta_2)$ and $(\beta_4 - \beta_3)$ are proportional to the first derivative of the ψ_3 function defined in Eq. (18). One easily proves that this term decays to zero extremely fast when the norm $|z_1|$ of its argument grows. In quantitative terms, we estimate

$$\frac{d\psi_3(z_1)}{dz} \propto \exp\left(-\sqrt{2}R'\right) \ . \tag{A4}$$

Since a typical value for the penetration depth of the seasonal thermal wave in the regolith layer is $l_s^1 \approx 15$ cm and the radius R of the bodies of interest may be as large as 100 meters, in such a case we obtain $|d\psi_3(z_1)/dz| \approx 10^{-400}$! While both the numerator and the denominator factors are of this order, their ratio is a finite number. Of course, without factorizing the $d\psi_3(z_1)/dz$ term, a precise evaluation of the complex number $E_{R'} \exp(i\delta_{R'})$ in the left–hand side of Eq. (A1) would be impossible. In our examples, therefore, we have developed the (h/R) term in Eq. (A3) up to the third power by using a Taylor expansion of the β_3 and β_4 functions.

Appendix B: plane–parallel solution

As explained in Appendix A, evaluating the seasonal semimajor axis drift (19) requires a special attention in the case of large bodies ($R' \gg 1$). In this limit, the plane–parallel (1–D) approximation of the heat diffusion problem becomes appropriate. This approach has been adopted by Rubincam (1995) and, using the same notations of this paper, by Vokrouhlický (1998b). The corresponding non–linearized theory has been developed by Vokrouhlický & Farinella (1998).

We have generalized the analysis given in Vokrouhlický (1998b) to account for: (i) the seasonal variant of the Yarkovsky effect; and (ii) the layered structure of the bodies studied in this paper. The final formula for the semimajor axis drift due to the seasonal component of the Yarkovsky effect is identical with Eq. (19), provided the $E_{R'} \exp(i\delta_{R'})$ function reads

$$\frac{E_{R'} \exp(i\delta_{R'})}{1+\chi} = -\frac{1}{1 - \Theta\sqrt{-\frac{i}{2}} \frac{1+\xi_{12}\exp\left(2\sqrt{-i}h'\right)}{1-\xi_{12}\exp\left(2\sqrt{-i}h'\right)}} \ , \tag{B1}$$

keeping the same notations as above, with

$$\xi_{12} = \frac{\xi_1 - \xi_2}{\xi_1 + \xi_2} \tag{B2}$$

[obviously, the dependence on R' has disappeared from Eq. (B1)]. Interestingly, formula (B1) can be evaluated without any numerical problems and can be used to check the quality of the approximation discussed in Appendix A. Results based on (B1) are shown in Fig. 2 as dashed curves. When $R' \gg 1$, we note a fairly good match with the complete solution (solid line), while at small sizes ($R' \leq 1/\xi_1$) the plane–parallel approximation of course fails.

References

Boley B.A., J.H. Weiner, 1960, Theory of Thermal Stresses. J. Wiley and Sons, New York

Bottke W.F., D.P. Rubincam, J.A. Burns, 1999, Icarus, in press

Brown R.H., Matson D.L., 1987, Icarus 72, 84

Dobrovolskis A.R., Burns J.A., 1980, Icarus 42, 422

Farinella P., Vokrouhlický D., Hartmann W.K., 1998, Icarus 132, 378

Farinella P., Vokrouhlický D., 1999, Sci 283, 1507

Genge M.J., Grady M.M., 1999, Meteoritics Planet. Sci. 34, 341

Hartmann W.K., Farinella P., Vokrouhlický D., et al., 1999, Meteoritics Planet. Sci. 34, A161

Langseth M.G., Keihm S.J., Chute J.L., 1973, Heat flow experiments. In: Apollo 17 – Preliminary Science Report. NASA SP–330

Lee P., 1996, Icarus 124, 181

Presley M.A., Christensen P.R., 1997, J. Geophys. Res. 102, 6551

Rabinowitz D.L., 1993, ApJ 407, 412

Rabinowitz D.L., 1994, Icarus 111, 364

Rubincam D.P., 1995, J. Geophys. Res. 100, 1585

Rubincam D.P., 1998, J. Geophys. Res. 103, 1725

Sitarski G., 1991, AJ 104, 1226

Vokrouhlický D., 1998a, A&A 335, 1093

Vokrouhlický D., 1998b, A&A 338, 353

Vokrouhlický D., 1999, A&A 344, 362

Vokrouhlický D., Farinella P., 1998, AJ 116, 2032

Vokrouhlický D., Farinella P., 1999a, In: The Impact of Modern Dynamics in Astronomy. Proceedings of the IAU Colloquium No. 172, Kluwer, Dordrecht, in press

Vokrouhlický D., Farinella P., 1999b, Nat, submitted

Wechsler A.E., Glaser P.E., Little A.D., Fountain J.A., 1972, In: Lucas J.W. (ed.) Thermal Characteristics of the Moon. MIT Press, Cambridge, p. 215

Wetherill G., 1985, Meteoritics 20, 1

Yeomans D., 1992, AJ 104, 1266

Yomogida K., Matsui T., 1983, J. Geophys. Res. 88, 9513